ELSEVIER

Journal of Nuclear Materials 276 (2000) 1–12

journal of nuclear materials

www.elsevier.nl/locate/jnucmat

The primary damage state in fcc, bcc and hcp metals as seen in molecular dynamics simulations

D.J. Bacon*, F. Gao, Yu.N. Osetsky

Materials Science and Engineering, Department of Engineering, The University of Liverpool, Brownlow Hill, Liverpool L69 3GH, UK

Abstract

Recent progress in the use of molecular dynamics (MD) to investigate the primary state of damage due to displacement cascades in metals is reviewed, with particular emphasis on the influence of crystal structure. Topics considered include the effect on defect formation in pure metals and alloys of primary knock-on atom (PKA) energy and irradiation temperature. An earlier empirical relationship between the production efficiency of Frenkel pairs and cascade energy is seen to have wide validity, and the reduction in efficiency with increasing irradiation temperature is small. Crystal structure has little effect on the defect number. In terms of the development of models to describe the evolution of radiation damage and its role in irradiation-induced changes in material properties, the important parameters are not only the total number of Frenkel defects per cascade but also the distribution of their population in clusters and the form and mobility of these clusters. Self-interstitial atoms form clusters in the cascade process in all metals, and the extent of this clustering does appear to vary from metal to metal. Vacancy clustering is also variable. The mobility of all clusters depends on their dislocation character and thus on the crystal structure and stacking fault energy. It is shown that computer simulation can provide detailed information on the properties of these defects.

1. Introduction

This paper is concerned with the number, arrangement and nature of the defects created inhomogeneously in space and time in metals subjected to radiation that produces displacement cascades. The cascade process occurs with length and time scales of the order of nm and ps, respectively, and is ideally suited to study by atomic-scale computer simulation using the method of molecular dynamics (MD). The defects created in cascades form the 'primary state' of damage and their subsequent evolution gives rise to important changes in the engineering properties of metals, and so understanding and predicting these are crucial for assessing material performance in irradiation environments. The evolution can occur over long periods of time with a characteristic length scale consistent with the evolving microstructure, and so is well-suited to continuum and/or stochastic Monte Carlo modelling. These are methods to be addressed by other authors in this volume. It must be noted, however, that the input parameters for such treatments require quantitative knowledge of not only the number of the defects formed in the primary state but also their distribution and properties, and the ways these may vary from metal to metal. This is where atomic-scale computer simulation can make a unique contribution.

Displacement cascades are formed by primary knock-on atoms (PKAs) that have a kinetic energy of more than a few hundred eV. As has been reviewed elsewhere [1–9], atomic-scale computer simulation has confirmed early ideas based on binary-collision concepts (e.g. [10]) that a cascade exhibits two main stages as it evolves with time. The first is a ballistic or collision phase lasting a few tenths of a ps, during which the energy of the PKA is distributed by multiple collisions among many atoms, with the result that they leave their lattice sites. This creates a central disordered core surrounded by regions of crystal displaced outwards. In the second, 'thermal-spike' phase lasting several ps, the kinetic and potential components of the crystal energy

* Corresponding author. Tel.: +44-151 794 4662; fax: +44-151 794 4675.

E-mail address: djbacon@liv.ac.uk (D.J. Bacon)

0022-3115/00/$ - see front matter
PII: S0022-3115(99)00165-8

attain equilibrium with each other and the hot disordered core initially acquires some liquid-like characterisitics. During this phase, the majority of the displaced atoms in the outer regions return by athermal relaxation to lattice sites in less than one ps, but strong disorder persists in the core for a longer time (several ps). The atoms that are unable to regain lattice sites during this final stage become self-interstitial atoms (SIAs) at the periphery of the core and, together with the vacant sites formed when the core crystallises, represent the main cascade contribution to the primary damage state. Individual replacement-collision sequences can be ejected early on during the ballistic phase, but SIAs created by these events represent only a minor part of the total population of Frenkel pairs produced by cascades at lattice temperatures where focused chains are difficult to establish.

Simulation studies of displacement cascades have now been made for a variety of metals under a fairly wide range of conditions. The results to be described in the following sections are concerned with topics such as the effects on defect production efficiency of PKA energy and irradiation temperature, and the proportion of defects formed as clusters in the cascade process itself, the nature of these clusters and their mobility. We shall follow the theme of this Workshop by trying to establish evidence for similarities and differences between metals with the bcc, fcc and hcp crystal structures.

2. The effect of PKA energy and crystal structure on defect number

Kinchin and Pease [11] obtained the first clear theoretical assessment of defect production in displacement cascades by deriving a simple relationship between the number, N_F, of SIA-vacancy pairs, i.e. Frenkel defects, created by a cascade and the kinetic energy, E_p, of the PKA. It was subsequently revised by Norgett et al. [12] to give the standard formula for estimating the displacements per atom (DPA) in irradiated metals [13]

$$N_{NRT} = 0.8E_{dam}/2\bar{E}_d, \tag{1}$$

where N_{NRT} is the value of N_F in the Norgett, Robinson and Torrens (NRT) formulation, $\bar{E}_d$ the value of the threshold displacement energy averaged over all crystallographic directions and E_{dam} is the damage energy available for elastic collisions, i.e. E_p with inelastic losses subtracted. (Since electronic losses have not been included in most MD simulations, the replacement of E_{dam} by E_p in Eq. (1) is appropriate for comparing its predictions with N_F obtained from MD [2].) The binary collision model on which the NRT formula is based does not accurately describe atomic interactions in the thermal spike and is not suitable for modelling the actual configuration defects adopt. MD simulations, on the other hand, use interatomic potentials fitted to many of the equilibrium and defect properties of metals and do offer a more realistic description of all stages of the cascade process.

All the MD simulations to date, starting with the early simulations of cascades in tungsten [14], show that defect production by displacement cascades in metals is not as efficient as predicted by the NRT formula. In fact, N_F is typically only 20–40% of N_{NRT} for a given cascade energy when E_p is larger than about 1–2 keV. By considering MD-generated N_F data for several metals, it was shown in [2] that a new empirical relationship between N_F and E_p gives a good fit to the simulation data for E_p up to either 5 or 10 keV

$$N_F = A(E_p)^m, \tag{2}$$

where A and m are constants which are weakly dependent on the material and temperature. The applicability of Eq. (2) over a wider energy range is now shown in Fig. 1 by using more recent data for N_F obtained for E_p up to 10 keV for Cu [15], α-Ti [16] and Ni_3Al [17], 20 keV for α-Zr [16] and 40 keV for α-Fe [18]. Each data point is the mean N_F value for at least four cascades at that energy and all the data were obtained for simulations of model crystals at a

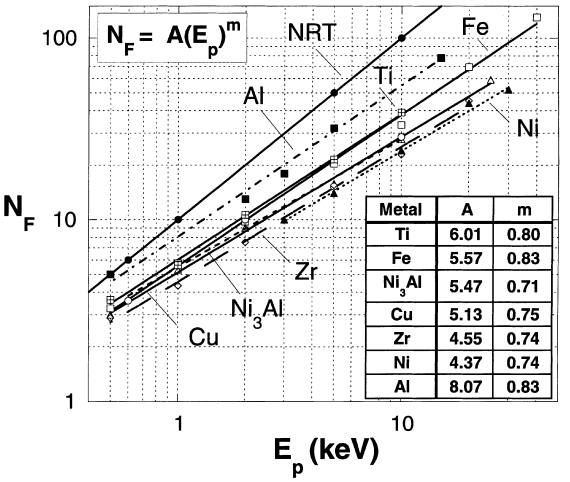

Fig. 1. Log–log plots of N_F vs E_p for Ni_3Al and the pure metals Cu, Fe, Ti and Zr at 100 K, and Al and Ni at 10 K, demonstrating the power-law dependence of Eq. (2) in the text. The inset table shows the values of m and A (with E_p in keV) obtained with the best-fit lines shown in the figure. The data for Al and Ni were kindly supplied by Almazouzi et al. [20].

temperature of 100 K. To extend the plot further, we have included data for four 40 keV cascades in α-Fe obtained by Stoller [19], and have added the value of N_F reported for 25 keV cascades in Cu at 10 K [5]. Very recently, Almazouzi et al. [20] have simulated cascades in Al and Ni at 10 K, with E_p up to 15 and 30 keV, respectively, and their data for N_F are included in Fig. 1.

The functional form of the power law (Eq. (2)) can be seen to provide an excellent fit to the data over a wide energy range. We include in Fig. 1 a line showing the NRT estimate for N_F assuming an $\bar{E}_d$ value of 40 eV. It clearly demonstrates the reduced efficiency with which simulated cascades produce Frenkel defects in comparison with the NRT prediction. This reduction occurs because most SIAs are produced at the periphery of the disordered core, rather than at the end of focused collision chains, and their close proximity to the vacancies and the high kinetic energy of the core during the thermal spike assist SIA-vacancy recombination. The MD data are consistent with experiments that imply that defect production efficiency in pure metals and alloys under cascade-producing irradiation with ions and neutrons is approximately one quarter of the NRT value [21–23].

Two other features are clear. First, the value of N_F has no obvious dependence on the crystal structure. Al, Cu and Ni are fcc, α-Fe is bcc, α-Ti and α-Zr are hcp and Ni_3Al has the ordered $L1_2$ structure. This is an important result because it implies that any generic differences observed experimentally between the damage microstructure in metals are not due to differences in defect production efficiency in the cascade process itself. Second, the differences in N_F that do exist between the metals appear to be due solely to the atomic mass, for N_F is highest in Al, followed by Ti and Fe. It can be seen from the table inserted in Fig. 1, that as the atomic mass increases, parameter A in Eq. (2) decreases, suggesting either an enhancement of recombination due to thermal spike effects or a scaling law arising from an increase in $\bar{E}_d$. Furthermore, the exponent m in the power-law relationship also reflects a dependence on the atomic mass of the metal. It is approximately 0.8 for Al, Ti and Fe, and nearer 0.75 for the others metals. As suggested by Stoller [19] and Almazouzi et al. [20], for example, the higher value for the lighter elements may reflect the attempt to fit Eq. (1) across the whole range of E_p, because as cascade energy increases, there is an increased tendency for cascades to become more diffuse and break up into sub-cascades. Since one cascade produces fewer defects on average than two separate cascades of the same total energy, sub-cascade formation would lead to an increase in the gradient of the plots in Fig. 1. This transition occurs at lower energy in the lighter metals, and can be discerned in the data for Al and Fe plotted in Fig. 1.

3. Defect production in alloys

Although most simulations of displacement cascades in metals have modelled pure elements, there has been some investigation of cascade effects in alloys and we touch on this briefly. The widest study reported on the effects of alloying elements in solution on cascades was by Deng and Bacon [24], who modelled cascades of up to 2 keV in energy in copper containing up to 15 at.% gold in solution. The atomic mass of Au is about three times that of Cu, and its presence decreased the length of focused displacement events in the ballistic phase and thereby enhanced the intensity and lifetime of the disorder and temperature during the thermal spike. However, despite this marked effect, the principal result was that N_F did not depend on the alloy composition, at least for the E_p range considered.

Calder and Bacon [25] carried out a similar study of cascades of 1, 2, 5 and 20 keV energy in Fe–Cu alloys containing 1% copper in solution. Six events at each energy were generated in order to provide adequate statistics. The aim was to see if N_F is affected by the presence of copper in solution and if cascades change either the cluster distribution of copper or produce clusters of copper atoms in association with point defects. The number of Frenkel pairs formed in the alloy was similar to that in pure iron, as may be expected in view of the results in [24] and the similar atomic mass and size of copper and iron. Furthermore, no evidence was found for significant Cu–Cu clustering during the cascade process itself, as would have been expected if cascade-assisted nucleation of copper precipitates occurs. The Cu–Cu binding energy is too small and the cascade lifetime too short.

Displacement cascades in ordered alloys produce numbers of Frenkel pairs, which, as seen in Fig. 1 for Ni_3Al, are comparable with those formed in pure metals. In addition, disorder occurs when either sites in the sub-lattices become occupied by atoms of the wrong type (known as antisite defects) or crystalline order is not restored and an amorphous structure is formed, and zones of either disordered crystal or amorphous structure are the dominant product of cascade damage in such materials [26–30]. Computer simulations have been used to investigate both aspects, e.g. [17,29–31] and [32–34]. Studies [17,29] of cascades in Ni_3Al show that instead of a declining production efficiency with increasing cascade energy, as discussed above for Frenkel pairs, the number of antisite defects per cascade, N_{AS}, actually increases with increasing E_p. A power law applies, but with an exponent of 1.25, in contrast to the value of approximately 0.75 found for N_F. The zone of antisites largely corresponds with the 'molten' core [29,30], demonstrating the importance of the thermal spike.

4. The formation of interstitial clusters in cascades

4.1. The fraction of interstitials formed in clusters

If point defects form clusters, rather than remain single, in the cascade process, their behaviour and role in subsequent evolution of the microstructure are affected (e.g. [35–40]). It is therefore of interest that MD simulations indicate that a significant fraction of the interstitial population created in cascades is produced in clusters. This is consistent with the experimental measurement of diffuse X-ray scattering in copper irradiated with neutrons at 4.6 K [41]. The grouping of SIAs into clusters is significant because these defects are thermally stable and, if they can migrate away from their parent cascades, should be absorbed preferentially at sinks such as dislocations and boundaries. Furthermore, the form of this migration depends on the cluster size (see Section 4.3). Vacancy clusters, in contrast, are not stable and dissociate into individual point defects at high enough temperature. These features affect the form and temperature-dependence of the accumulation of damage microstructure and have been formulated within the 'production bias model' of damage evolution [35–40].

As far as interstitials are concerned, computer simulation shows that some clusters are created quite early on in the cascade process during the transition from the collision to thermal-spike phases, whereas others arise during the thermal spike by short-range diffusion. Cluster formation in the former circumstance seems to occur when groups of atoms being displaced outwards from the cascade centre in the initial shock wave are pushed into interstitial sites from which they cannot escape; clustering by the latter mechanism occurs as a result of reorganisation driven by the large elastic interaction among neighbouring interstitials. We shall not distinguish between the two processes in the following. The probability of clustering and the size of the largest clusters tend to increase with increasing PKA energy, and a higher proportion of SIAs than vacancies form clusters. These features hold true for all the metals studied to date and are demonstrated by the histograms in Fig. 2(a) and (b) for the cluster statistics of cascades of up to 20 keV in energy in α-Zr [16] and 40 keV in energy in α-Fe [18], respectively. For these data, an SIA or a vacancy is a member of a cluster if it has at least one partner in a nearest-neighbour position. The data for vacancies will be considered further in the Discussion (Section 6).

Although the conclusion of the preceding paragraph holds generally, the results of MD simulations indicate that differences may exist between different metals. For example, it is seen in Fig. 2 that the clusters formed by interstitials tend to be larger than those formed by vacancies in iron, but not in zirconium. Furthermore,

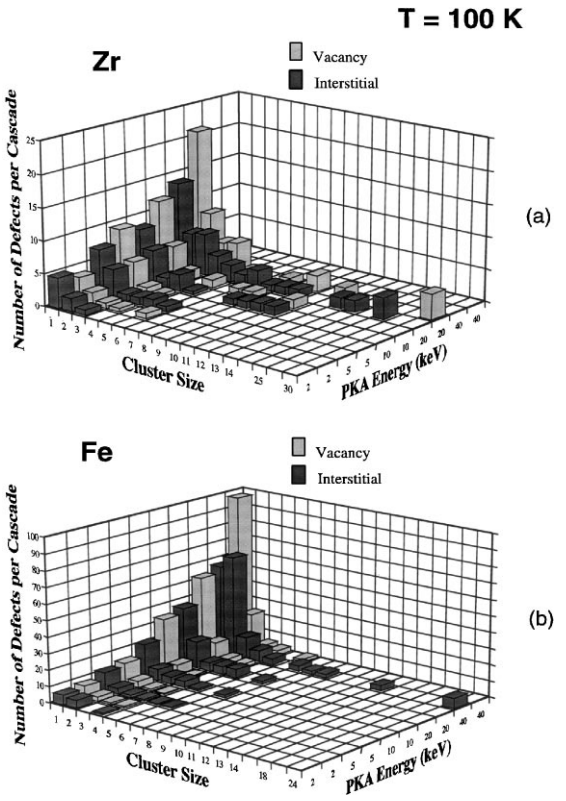

Fig. 2. Data for the number of SIAs and vacancies in clusters per cascade as a function of cascade energy in: (a) α-zirconium and (b) α-iron at 100 K. The data were obtained by averaging over all cascades at each energy.

the clustered fraction of interstitials created in the cascade process appears to have some dependence on the metal, as shown in Fig. 3 by the fraction, f_i^{cl}, of

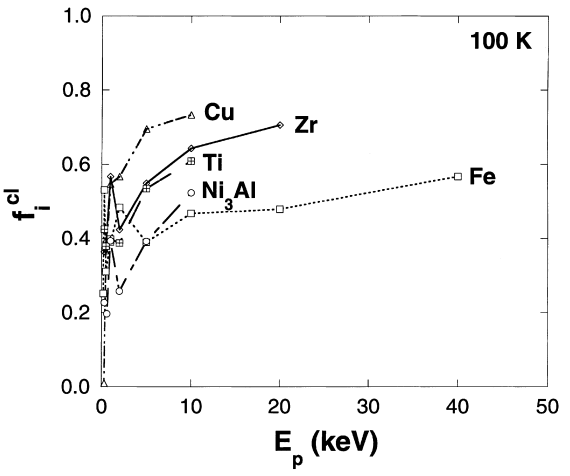

Fig. 3. The fraction, f_i^{cl}, of SIAs that survive in clusters of two or more in Cu, α-Fe, α-Ti, α-Zr and Ni_3Al at 100 K.

interstitials that exist in clusters of size two or larger in the metals Cu [15], α-Fe [18], α-Ti, α-Zr [16] and Ni_3Al [17] at 100 K. The clustered fraction increases strongly at low energy in the transition from single displacement events to true cascade phenomena, and above this there is a smaller variation with PKA energy. The increase with increasing energy probably reflects the increasing importance of the two mechanisms mentioned in the preceding paragraph.

It can be seen that f_i^{cl} varies from metal to metal, being highest in copper and lowest in iron, and does not seem to be related to the differences in the total number of Frenkel pairs produced (Fig. 1). Although only five metals are considered, the data of Fig. 3 suggest that the difference in clustering behaviour among the metals may be influenced by the crystal structure. For example, f_i^{cl} values are similar in the two hcp metals Ti and Zr, despite the significant differences in N_F, possibly because SIAs in the hcp metals have high mobility within the basal planes relative to that for motion between these planes [16,42,43], and this may affect their ability to cluster during the thermal spike. Similarly, the presence of the large number of antisite defects in the disordered core of cascades in ordered alloys may restrict SIA movement and reduce the probability of cluster formation [17]. The difference between iron and copper may arise from the larger number of close-packed directions in the latter (six compared with four): these are the directions along which interstitial atoms migrate easily during and immediately after the thermal spike. However, confirmation of these ideas must await studies of a wider range of metals.

4.2. The glissile–sessile nature of interstitial clusters

Many of the clustered SIAs formed in cascades simulated by MD have high mobility in the context of the time-scale of the simulations, i.e. they can migrate over sizeable distances (on the atomic scale) in times of the order of tens of ps. The high jump rate of single interstitials had been expected because of the low value of their migration energy deduced from the temperature of stage I in recovery experiments, but an appreciation of the mobility of SIA clusters has arisen from the MD simulations. We shall return to this point in the following section, and remark for the moment that the SIA clusters found to be mobile exhibit a morphology akin to that of perfect dislocation loops and are therefore 'glissile'.

Not all interstitial clusters seen in MD simulations of cascades have a glissile form, however. 'Sessile' clusters have been reported in both titanium [42] and zirconium [16,44], and recent work has revealed the extent to which they occur in iron [18]. Some are formed early on in the cascade by ballistic events and others arise later due to SIA interaction in the thermal spike. They are not restricted in size. In the case of zirconium, for example, the largest interstitial cluster found in all the simulations for E_p up to 20 keV consisted of 25 defects and had a sessile form [16].

We must distinguish here between clusters which are stable and intrinsically sessile, such as those based on faulted Frank loops in the fcc metals, and those formed by metastable arrangements of SIAs that do not reorganise into a stable, glissile form by the end of the thermal spike. The latter are the topic of this section. Their possible significance lies in the fact that in a damage flux, they do not migrate away from their parent cascade at the end of the thermal spike and may actually behave as sinks for mobile defects in their own right, thereby allowing extended defects to grow in their place of birth. Hence, a clear understanding of the properties of these defects is required, such as their lifetime for conversion to a glissile form at different temperatures and their stability in relation to interaction with mobile defects.

To illustrate the extent of metastable, sessile cluster formation, we consider data for interstitials created by cascades with energy between 5 and 40 keV in α-iron at 100 and 600 K [18]. At least four simulations were carried out at each energy and temperature, and were stopped when the cascade zone had cooled to the ambient temperature (after about 20–30 ps). The glissile and sessile components of the clustered fraction of SIAs were then identified from their morphology. The mean values of the fraction of interstitials in sessile clusters are plotted as a function of cascade energy in Fig. 4, where the bars denote the standard error. It is seen that across the energy range, between 30% and 50% of the clustered population have sessile character at the irradiation

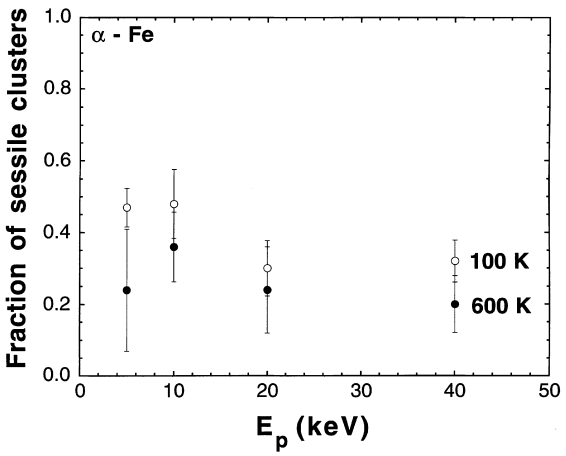

Fig. 4. The fraction of SIA clusters formed in a metastable sessile configuration by the end of the thermal spike phase as a function of PKA energy and irradiation temperature for cascades in α-iron [18].

temperature of 100 K. To illustrate the numbers involved at, say, 40 keV, 57% of the SIAs were in clusters of size two or more at 100 K and each cascade generated 24 such clusters on average. Of these, 17 were glissile and seven sessile, with sizes ranging from 2 up to 24 and 9, respectively, and average size of 2.9 and 3.2. Thus, over 30% of the clustered interstitials were found to be in a sessile form at this energy and irradiation temperature. We shall return to the data for 600 K in the next section.

The form of the metastable sessile clusters is very varied and depends on the crystal structure. In zirconium and titanium [16], for instance, small sessile clusters can be formed as a triangular arrangement of closely-packed atoms within one basal plane occupying a smaller number of lattice sites, e.g. six atoms and three sites, 10 atoms and six sites, 15 atoms and 10 sites, etc. Another, larger sessile arrangement of 25 SIAs was formed in a 20 keV cascade in zirconium and consisted of interstitial atoms spread over several basal and prism planes: it was stable over a simulation time of 120 ps. In iron, some sessile clusters arise from the attraction of mobile species that impinge on each other in positions that prevent instantaneous organisation into a stable, glissile loop. Others, possibly with the same number of defects, adopt a more open, three-dimensional structure. This is illustrated by two different versions of sessile di-interstitials reported in [45] and reproduced in Fig. 5. In Fig. 5(a), three atoms, shown as large circles, share one lattice site, shown by a smaller circle. The plane of the atoms is $\{1\,1\,1\}$, but is displaced slightly from the $\{1\,1\,1\}$ plane that passes through the vacant site. This cluster can form either directly in the early stages of a cascade or by the interaction and combination of two single defects during the thermal spike. The cluster in Fig. 5(b) arises from 12 atoms sharing 10 lattice sites, the latter consisting of four of the eight nearest neighbours and all six second-nearest neighbours of an atom in the bcc structure, as indicated by the dashed lines outlining a bcc cell. (The smallest circles in Fig. 5(b) represent sites in this cell that are occupied by atoms.) This symmetric, three-dimensional cluster was created in about half the cascades simulated and was formed well before the end of the thermal spike phase. Higher-order SIA clusters in α-iron exhibit more complicated variants of defects such as these [45].

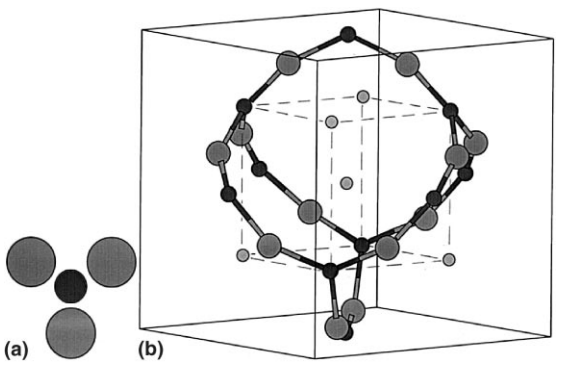

Fig. 5. Two versions of metastable di-interstitials created in cascade simulations of α-iron: (a) the large spheres represent atoms displaced to interstices and the smaller spheres represent vacant lattice sites and (b) the smallest spheres represent the sites of a bcc unit cell occupied by atoms. The defect in (a) is three atoms in a $\{1\,1\,1\}$ plane sharing one lattice site, whereas the one in (b) is 12 atoms sharing 10 sites.

4.3. The mobility of glissile interstitial clusters

As has been seen, MD simulations have demonstrated that the majority of interstitial clusters formed during the cascade process, and those that arise soon afterwards by the transformation of metastable clusters, are glissile, a property that is intimately related to their atomic structure. Detailed investigation of structure and mobility has been carried out for copper and iron in [46–50] using several different interatomic potentials, and a preliminary study for zirconium has been reported in [43]. A comprehensive review is presented elsewhere in this volume [50]. In qualitative terms, the properties do not depend on the type of interatomic potential used.

The glissile clusters in all the metals studied to date have the form of densely-packed, parallel crowdions, with the crowdion axis along a close-packed direction, i.e. $\langle 1\,1\,0\rangle$ in fcc, $\langle 1\,1\,1\rangle$ in bcc and $\langle 1\,1\,\bar{2}\,0\rangle$ in hcp. This form persists even in metals where the stable, single self-interstitial is a dumbbell rather than a crowdion. Some static visualisations of SIA clusters are plotted in earlier reviews of MD simulations of cascades [2,3,7,9] and the original papers [16,51]. Clusters of more than three SIAs exhibit thermally-activated, one-dimensional glide along the crowdion direction and only smaller clusters can change their glide direction. The larger clusters are akin to perfect dislocation loops with a Burgers vector **b** along the crowdion axis, so that their movement can be considered as thermally-assisted glide. During this motion they produce displacements of the atoms in the model crystallite, but analysis of this process has shown that it cannot be described as classical diffusion [49,50]. Nevertheless, some dynamical characteristics have been estimated by using MD to study the movement of the centre of gravity of the SIAs in moving clusters over periods of the order of nanoseconds. An important feature of motion is that the effective correlation factor is greater than one, i.e. a cluster that has moved by one step has a high probability of making the next step in the same direction. This effect increases at low temperature and is not yet understood, but is probably related to the response of crowdion clusters to specific phonons [49].

If the jump frequency for clusters containing from 2 to 91 $\langle 1\,1\,1\rangle$ crowdions in α-Fe at different temperatures

is analysed via an Arrhenius-like plot, the estimated 'activation energy' is within the range 0.022–0.026 eV for all clusters and is close to the migration energy of 0.023 eV estimated for the low-temperature $\langle 1\,1\,1\rangle$ crowdion mechanism [47]. Clusters of more than about 15–20 $\langle 1\,0\,0\rangle$ crowdions are also stable in this metal and describe small, perfect loops with $\mathbf{b} = \langle 1\,0\,0\rangle$ [48,49]. They show the same glissile behaviour as the $\langle 1\,1\,1\rangle$ clusters, but with a slightly higher activation energy of 0.028 eV. Two types of SIA cluster based on sets of $\langle 1\,0\,0\rangle$ dumbbells and $\langle 1\,1\,0\rangle$ crowdions can be stable in copper [48]. The former create Frank loops with $\mathbf{b} = 1/3\langle 1\,1\,1\rangle$, which are intrinsically sessile. The latter create glissile perfect loops and an Arrhenius treatment of MD data for their jump frequency at different temperatures gives an activation energy within the range 0.024–0.030 eV [48,50].

The data for α-Fe have been analysed by Barashev et al. [52] in order to compare the average jump frequency of the individual crowdions in a cluster with that of the cluster as a whole. The jump frequency of a cluster is found to be approximately equal to the average jump frequency of individual crowdions divided by their number. This is consistent with the interpretation that the movement of the centre of mass of an SIA cluster is the result of near-independent jumps of the individual crowdions. However, it should be stressed that there is more complexity in the mobility of SIA clusters in terms of size than represented in this simple picture. For example, when perfect loops with $\mathbf{b} = 1/2\langle 1\,1\,0\rangle$ in Cu grow beyond about 60–70 interstitials, they dissociate on their glide prism and this restricts thermally-activated motion, whereas the larger $\langle 1\,1\,1\rangle$ loops in Fe remain mobile [50,58].

5. The effect of irradiation temperature on defect production in cascades

Irradiation temperature has a significant effect on the evolution of radiation damage in metals because the motion of defects and the dissociation of their clusters are thermally-activated processes. In this section, however, we only consider the role of temperature on the production of damage in the cascade process itself. In most MD simulations reported in the literature, the PKA was generated in a lattice equilibrated at 100 K or less, and, although an early study of the effect of ambient bulk temperature, T_{irr}, on the number and distribution of defects in cascade damage in both copper and iron was reported in [15,51], the MD block in these simulations was treated as an adiabatic system. A more rigorous method to allow for heat to be extracted from the atoms at the outer layers of the MD block to match the temperature predicted for that region in a continuum with the same thermal characteristics as the atomic system has been developed in [53] and applied to defect generation in α-iron [18,53] and Ni_3Al [54].

The results for N_{F} as a function of irradiation temperature, T_{irr}, in α-Fe are plotted in Fig. 6, where each point is the mean for four cascades for $E_{\mathrm{p}} = 2$, 10, 20 and 40 keV and eight cascades for 5 keV, and the bars represent the standard error. The effect on N_{F} of increasing T_{irr} is small but clear: the number of defects produced decreases. A similar result holds for the effects of temperature on cascades in Ni_3Al [54], suggesting that the reduction in N_{F} with increasing T_{irr} does not depend on the metal. This effect is believed to be due to the increase in the lifetime of the thermal spike as T_{irr} increases (see plots in [53,54]), which allows more defect motion to take place before cooling and hence leads to more interstitial–vacancy recombination. Another contributory factor may be the reduction in the interstitial–vacancy separation because cascades tend to have a more compact form at higher temperature due to the shorter length of focused collision sequences.

The simulations reviewed in Section 3 show that the final number, N_{AS}, of antisite defects created by cascades in Ni_3Al at 100 K greatly exceeds the number of vacancies and interstitial atoms. This result holds at all temperatures and increasing T_{irr} actually enhances the production of antisite defects, particularly in the higher part of the temperature range [54].

The fraction, $f_{\mathrm{i}}^{\mathrm{cl}}$, of SIAs formed in clusters of size two or more during the cascade process was discussed as a function of metal and PKA energy in Section 4.1. Data obtained in [18,53] for cascades of between 5 and 40 keV in α-Fe are plotted together as a function of the irradiation temperature in Fig. 7. The points represent the mean values and the bars indicate the standard error. An increasing fraction of the decreasing population of interstitials forms clusters as temperature increases. A similar result is found for $f_{\mathrm{i}}^{\mathrm{cl}}$ in Ni_3Al [54]. This enhancement of SIA clustering under increasing T_{irr} is

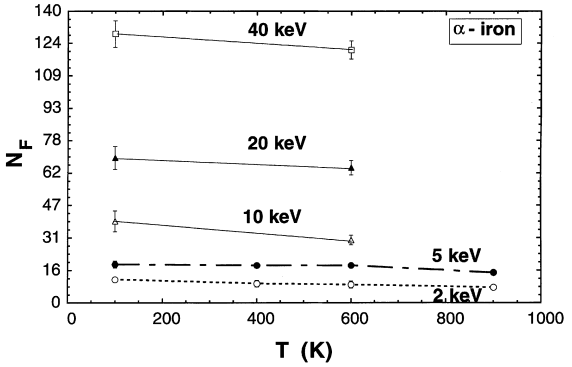

Fig. 6. Data for the number of Frenkel pairs produced per cascade as a function of PKA energy and irradiation temperature in α-iron [18,53].

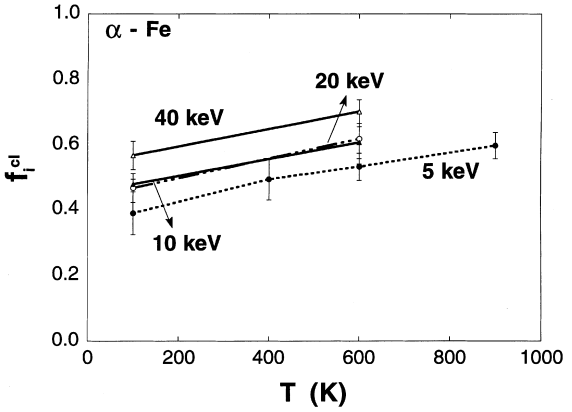

Fig. 7. Variation of the interstitial clustering fraction, f_i^{cl}, as a function of initial lattice temperature for cascades in α-iron [18,53].

believed to be due to the more compact form of a cascade and the longer lifetime of the thermal spike at the higher temperature. These effects result in smaller separation and greater mobility of the SIAs in this phase of cascade evolution.

It was noted in Section 4.2 that a significant fraction of the SIA clusters formed by cascades in α-Fe at 100 K has a metastable, sessile form. The fraction of such clusters is temperature dependent, however, as can be seen by comparing the data for $T_{irr} = 600$ K with that for 100 K in Fig. 4 [18]. The fraction of interstitials in clusters increases between 100 and 600 K, but the fraction of them in sessile clusters decreases, due to the higher probability of a transformation from sessile to glissile form in the thermal spike at the higher temperature. Nevertheless, the sessile fraction is still significant, and it may be remarked that the largest cluster (of 18 interstitials) generated in all of the cascades represented in Fig. 4 was sessile in form.

6. Discussion

The data presented in Section 2 for N_F lead to one of the key results to have emerged from MD simulations: there are only slight differences between different metals in terms of the efficiency of SIA and vacancy production in cascades. It may be concluded that differences observed in the response of metals to radiation damage in fluxes that create cascades arise in most cases from the properties of defects that affect the evolution of microstructure after the primary damage state. The empirical power law (Eq. (2)) relating N_F to the PKA energy E_p provides an excellent fit to the data generated by a large number of MD simulations of cascades in metals, thereby suggesting that it has wide applicability, irrespective of the crystal structure, over energy levels from a few hundred eV up to several tens of keV. (As noted in Section 2, however, Eq. (2) may no longer be strictly valid at high energies where sub-cascades form, because the defect number is then simply the sum of N_F for lower energy events.)

Another clear result to have been established by MD simulations of all metals is that SIA clusters form in the cascade process itself. Although the average size of these clusters is small – about three SIAs per cluster for 40 keV cascades in α-Fe (Section 4.2) – some individual clusters are large, containing up to several tens of SIAs. This is consistent with experimental evidence on average size from diffuse X-ray scattering [41] and the recent identification by transmission electron microscopy of interstitial dislocation loops in ion-irradiated copper [55].

In many of the MD simulations reported in the literature, the precise nature of the interstitial clusters has not been determined. However, in the cases where it has, many of the clusters are mobile and the recent MD simulations provide considerable insight into the nature of this mobility (Section 4.3). The ability to move arises from the clustered crowdion form of these extended defects. They have a form best described as small interstitial dislocation loops with 'perfect' Burgers vector **b** equal to $1/2\langle 1\,1\,0\rangle$ in fcc, $1/2\langle 1\,1\,1\rangle$ and $\langle 1\,0\,0\rangle$ in bcc and $1/3\langle 1\,1\,\bar{2}\,0\rangle$ in hcp. Although we have seen that their mobility decreases with increasing size, it should be noted that such perfect dislocation loops are intrinsically glissile with regard to motion on their glide prism. In contrast with this, if clusters form as faulted dislocation loops, such as $\mathbf{b} = 1/3\langle 1\,1\,1\rangle$ in fcc, $1/2\langle 1\,1\,0\rangle$ in bcc and $1/2\langle 1\,0\,\bar{1}\,0\rangle$ or $1/2[0\,0\,0\,1]$ in hcp, they are intrinsically sessile and cannot exhibit such motion. This essential difference between different clusters is summarised in Table 1. The observation of faulted interstitial loops has been reported in fcc metals and they have also been studied by MD, e.g. [48,50], but we are not aware of their observation in pure bcc metals, and in the hcp case

Table 1
The intrinsic glissile/sessile nature of defect clusters, both self-interstitial and vacancy, that have dislocation character in metals. A dislocation loop has a glide cylinder defined by the surface that contains both **b** and the line, and is intrinsically glissile on that surface if **b** is a lattice translation vector [56]

Bcc (e.g. α-Fe)	$\mathbf{b} = 1/2\langle 1\,1\,1\rangle$	Glissile
	$\mathbf{b} = \langle 1\,0\,0\rangle$	Glissile
Fcc (e.g. Cu)	$\mathbf{b} = 1/2\langle 1\,1\,0\rangle$	Glissile
	$\mathbf{b} = 1/3\langle 1\,1\,1\rangle$	Sessile
	SFT (vac only)	Sessile
Hcp (e.g. α-Zr)	$\mathbf{b} = 1/3\langle 1\,1\,\bar{2}\,0\rangle$	Glissile
	$\mathbf{b} = 1/2\langle 1\,0\,\bar{1}\,0\rangle$	Sessile
	Other **b**	Probably sessile

they only form on the basal planes when c/a is large [57]. This discussion demonstrates that stacking fault energy and crystal structure must be taken into account in assessing whether interstitial clusters are likely to be mobile or not.

It was shown in Section 4.2 (Fig. 4) that a significant fraction of the primary interstitial clusters created in cascade simulations of α-iron is found to have a sessile form, even at high irradiation temperature. These immobile defects do not have the intrinsically sessile nature of imperfect dislocations, but, were they to persist over long time-scales, could have important consequences for damage evolution. Their stability has therefore been investigated [45] by annealing a representative selection of them individually in an MD block for long periods (>1 ns) in order to study the temperature-dependence of their lifetime before transformation to the more stable, glissile form of $\langle 1\,1\,1\rangle$ crowdions. The lifetime, τ, of sessile clusters consisting of two, four or 13 SIAs is plotted against the reciprocal of the annealing temperature in Fig. 8. These defects transformed in well under 1 ns at temperatures in the range 500–900 K, with an activation energy for the transformation (given by the gradient of the line drawn on the plot) of about 0.35–0.55 eV. This implies that they should mainly affect the annealing of cascades rather than microstructure evolution in the long term. However, an eight-interstitial cluster based on the defect shown in Fig. 5(b) did not transform in the 1 ns simulations, even at 1500 K [45]. In view of this, the stability of this defect is currently under investigation using different interatomic potentials.

Although the lifetime of most sessile SIA clusters may be short, they can interact with glissile clusters formed in the same cascade. In fact, simulations reported in [45] provide an example where such an interaction leads to a change in the glide direction, i.e. **b**, of a moving cluster. Effects such as this may offer a way for SIA clusters which glide one-dimensionally to change the direction of their motion.

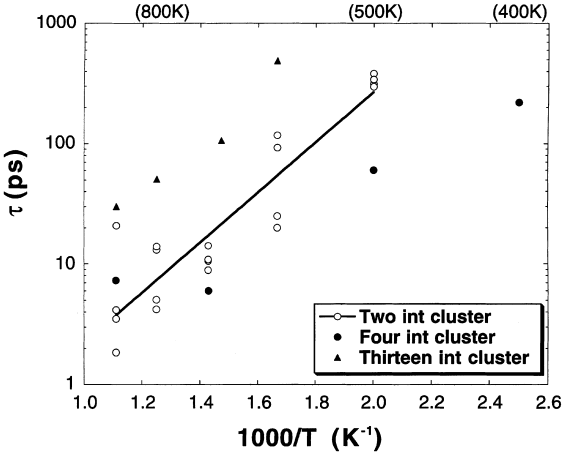

Fig. 8. The lifetime of several different metastable SIA clusters in α-iron as a function of annealing temperature [45].

One final point needs to be made before closing the discussion on SIA clusters. The data presented in Fig. 3 of Section 4.1 for the clustered fraction, f_i^{cl}, were derived for a minimum cluster size of two interstitials. However, this disguises the sensitivity of the relationship between f_i^{cl} and E_p to this minimum size, because low-energy cascades do not produce large clusters (see Fig. 2). This effect may have important consequences in the light of the evidence from MD that the dimensionality of the motion of clusters depends on their size, i.e. clusters of size three or less can change their glide direction and hence migrate three-dimensionally (Section 4.3), and this controls the kinetics of their interaction with other components of the microstructure [40]. To illustrate the influence of PKA energy on the fraction of SIAs in three- or one-dimensional clusters, we present in Fig. 9 values for f_i^{cl} versus E_p in copper and iron at 100 K for the cases where the minimum cluster size is either two, three or four SIAs. (The data were extracted from the data sets generated by the cascade modelling reported in [15,18].) The proportion of primary SIA clusters that glide in one direction only is predicted to be smaller in iron than copper, and it can be seen that f_i^{cl} is very sensitive to the choice of minimum cluster size in the lower part of the energy spectrum in copper. These data demonstrate the way in which atomic-scale modelling is able to provide detailed information for use in models of damage evolution.

In the context of a discussion of defect mobility, it should also be noted that *vacancy* clusters that have the form of dislocation loops with a perfect Burgers vector are also intrinsically glissile, as summarised in Table 1. In a clear demonstration of this, it has been found recently by MD simulation that the mobility of perfect vacancy loops with $\mathbf{b} = 1/2\langle 1\,1\,0\rangle$ and $1/2\langle 1\,1\,1\rangle$ in Cu and α-Fe, respectively, is only slightly lower than that of clusters of the same number of interstitial crowdions [58]. This result is illustrated by the data for the jump frequency of vacancy and SIA loops as a function of temperature in Fe in Fig. 10. Hence, the motion of perfect vacancy loops should not be neglected in the modelling of damage evolution, irrespective of the crystal structure. If, on the other hand, collapsed vacancy clusters have a partial Burgers vector or form stacking fault tetrahedra, they are intrinsically sessile (Table 1). Also, if vacancy clusters do not collapse to a dislocation structure, as seen most commonly in MD simulations of cascades, they cannot move by glide, only by diffusion of individual members of the cluster.

In relation to the last point, we have not addressed in any detail the clustering of vacancies in cascades, though the form and stability of the vacancy component are important elements in damage evolution. Clusters of

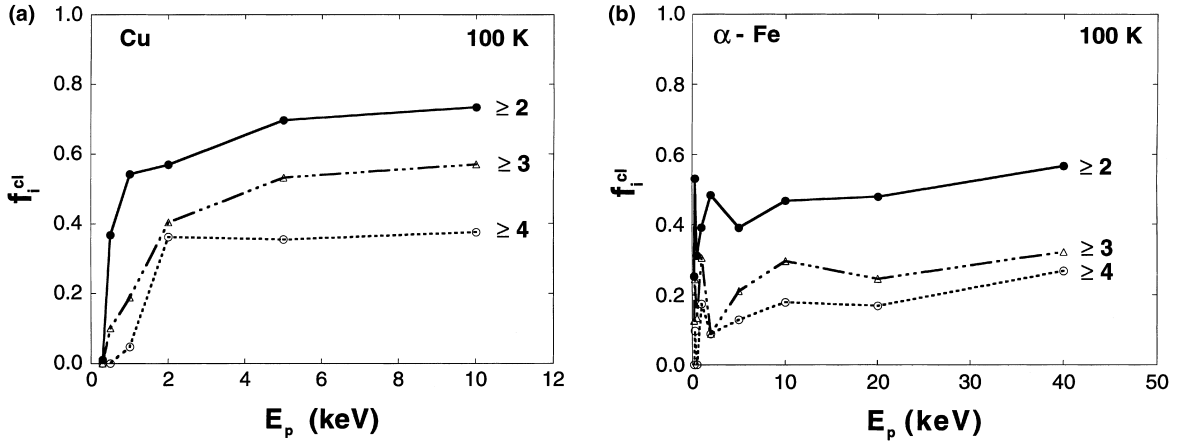

Fig. 9. The fraction, f_i^{cl}, of SIAs that survive in clusters of two or more, three or more, and four or more in: (a) copper and (b) α-iron at 100 K.

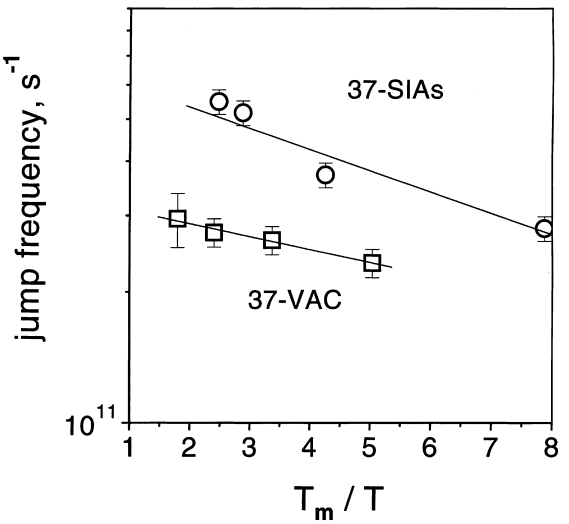

Fig. 10. Jump frequency of the centre of mass of clusters consisting of either 37⟨1 1 0⟩ crowdions or 37 vacancies in α-iron at different temperatures [58].

vacancies do occur within the core of cascades, as seen in the data for iron and zirconium in Fig. 2. The extent of vacancy clustering, like that of interstitials, varies from metal to metal, and larger vacancy clusters are formed in the hcp metal α-Zr than in bcc Fe at the same cascade energy. However, it is not clear to what extent this depends on the crystal structure, as opposed to atomic mass.

One issue of concern for MD modelling of displacement cascades is that the vacancy clusters observed in most simulations are not collapsed into forms with dislocation character, despite the fact that vacancy dislocation loops and stacking fault tetrahedra a few nm in size are formed by cascades in many metals and are readily observed by transmission electron microscopy of thin, ion-irradiated foils [59,60]. As discussed in [3,61], there is evidence from MD modelling of cascades near a surface that the mechanism involved in the formation of some collapsed vacancy clusters in ion-irradiated thin foils may not apply to conditions in the bulk, but this cannot account for all the loops and tetrahedra observed. This raises the question as to whether the short-range, many-body interatomic potentials used for the vast majority of cascade simulations provide a suitable framework for describing atomic behaviour when a super-saturation of vacancies exists. There has been little progress in this area since [3], although very recent simulations [50,58,62,63] of vacancy clusters in both copper and iron using short-range, equilibrium potentials of many-body form and long-range, non-equilibrium pair potentials have shown that some of the properties of these clusters are sensitive to the nature of the interatomic potential.

The development of potentials that would offer an improvement for all aspects of cascade and defect simulation in metals is undoubtedly a topic for future research. The many-body interatomic potentials used in the cascade simulations reviewed here are suitable for the scale of modelling required, i.e. MD cells containing $\sim 10^4$–10^6 atoms and times of typically tens of ps, but impose isotropy, i.e. absence of directionality, in the atomic bonds. It is not known to what extent a more accurate description of interatomic forces for, say, the transition metals would affect the production of defects by the cascade process. Most probably, the ballistic phase and the early part of the thermal-spike phase would not be influenced to any significant extent, but angular forces could affect defect behaviour later on. It seems unlikely that they would seriously alter the general

trends for N_F and f_i^{cl} discussed here, but they could influence SIA mobility and clustering. This could come about, for instance, if the single $\langle 1\,1\,0\rangle$-dumbbell interstitial in the bcc metals does not actually adopt the $\langle 1\,1\,1\rangle$ crowdion form when in clusters of two or more, which is the configuration found with the potentials currently in use.

Acknowledgements

This research was supported by research grants from the Engineering and Physical Sciences Research Council, Magnox Electric plc and the University of Liverpool.

References

[1] T. Diaz de la Rubia, M.W. Guinan, A. Caro, P. Scherrer, Rad. Eff. Def. Sol. 130&131 (1994) 39.
[2] D.J. Bacon, A.F. Calder, F. Gao, V.G. Kapinos, S.J. Wooding, Nucl. Instrum. and Meth. B 102 (1995) 37.
[3] D.J. Bacon, A.F. Calder, F. Gao, Rad. Eff. Def. Sol. 141 (1997) 283.
[4] T. Diaz de la Rubia, M.W. Guinan, Mater. Res. Forum 97–99 (1992) 23.
[5] T. Diaz de la Rubia, W.J. Phythian, J. Nucl. Mater. 191–194 (1992) 108.
[6] R.S. Averback, J. Nucl. Mater. 216 (1994) 49.
[7] D.J. Bacon, T. Diaz de la Rubia, J. Nucl. Mater. 216 (1994) 275.
[8] D.J. Bacon, in: H.O. Kirchner, L.P. Kubin, V. Pontikis (Eds.), Computer Simulation in Materials Science, Kluwer Academic, Dordrecht, 1996, p. 189.
[9] D.J. Bacon, A.F. Calder, F. Gao, J. Nucl. Mater. 251 (1997) 1.
[10] A. Seeger, in: Proceedings of the Second United Nations Conference on Peaceful Uses of Atomic Energy, IAEA, Vienna, 1958, p. 250.
[11] G.H. Kinchin, R.S. Pease, Rep. Prog. Phys. 18 (1955) 111.
[12] M.J. Norgett, M.T. Robinson, I.M. Torrens, Nucl. Eng. Design 33 (1975) 50.
[13] Standard E521, ASTM Annual Book of Standards, 1989.
[14] M.W. Guinan, J.H. Kinney, J. Nucl. Mater. 103&104 (1981) 1319.
[15] W.J. Phythian, A.J.E. Foreman, R.E. Stoller, D.J. Bacon, A.F. Calder, J. Nucl. Mater. 223 (1995) 245.
[16] S.J. Wooding, L.M. Howe, F. Gao, A.F. Calder, D.J. Bacon, J. Nucl. Mater. 254 (1998) 191.
[17] F. Gao, D.J. Bacon, Philos. Mag. A 71 (1995) 43.
[18] F. Gao, D.J. Bacon, unpublished work.
[19] R.E. Stoller, in: I.M. Robertson, L.E. Rehn, S.J. Zinkle, W.J. Phythian (Eds.), Proceedings of the Symposium on Microstructure of Irradiated Materials, vol. 373, MRS Pittsburgh, 1995, p. 21.
[20] A. Almazouzi, M.J. Caturla, T. Diaz de la Rubia, M. Victoria, EPFL Supercomputing Review, No. 10, Swiss Fed. Inst. Of Tecnology, 1998, p. 10.
[21] R.S. Averback, R. Benedek, K.L. Merkle, Phys. Rev. B 18 (1978) 4156.
[22] P. Jung, J. Nucl. Mater. 117 (1983) 70.
[23] J.H. Kinney, M.W. Guinan, Z.A. Munir, J. Nucl. Mater. 122/123 (1984) 1028.
[24] H.F. Deng, D.J. Bacon, Phys. Rev. B 54 (1996) 11376.
[25] A.F. Calder, D.J. Bacon, in: T. Díaz de la Rubia et al. (Eds.), Proceedings of the Symposium on Microstructure Evolution During Irradiation, vol. 439, MRS, Pittsburgh, 1997, p. 521.
[26] D.I. Potter, in: F.V. Nolfi (Ed.), Phase Transformations During Irradiation, Applied Science, Barking, 1983, p. 213.
[27] M.L. Jenkins, J. Nucl. Mater. 216 (1994) 124.
[28] N.Q. Lam, P.R. Okamoto, M. Li, J. Nucl. Mater. 251 (1997) 89.
[29] F. Gao, D.J. Bacon, Philos. Mag. A 71 (1995) 65.
[30] T. Diaz de la Rubia, A. Caro, M. Spaczer, Phys. Rev. B 47 (1993) 11483.
[31] N.V. Doan, R. Vascon, Rad. Eff. Def. Sol. 141 (1997) 363.
[32] M. Spaczer, A. Caro, M. Victoria, T. Diaz de la Rubia, Phys. Rev. B 50 (1994) 13204.
[33] H. Zhu, R.S. Averback, M. Nastasi, Philos. Mag. A 71 (1995) 735.
[34] M. Spaczer, A. Almazouzi, R. Schaublin, M. Victoria, Rad. Eff. and Def. Sol. 141 (1997) 349.
[35] C.H. Woo, B.N. Singh, Philos. Mag. A 65 (1992) 889.
[36] S.J. Zinkle, B.N. Singh, J. Nucl. Mater. 199 (1993) 173.
[37] H. Trinkhaus, V. Naundorf, B.N. Singh, C.H. Woo, J. Nucl. Mater. 210 (1994) 244.
[38] B.N. Singh, J.H. Evans, J. Nucl. Mater. 226 (1995) 277.
[39] B.N. Singh, S.I. Golubov, H. Trinkhaus, A. Serra, Yu.N. Osetsky, A.V. Barashev, J. Nucl. Mater. 251 (1997) 107.
[40] S.I. Golubov, B.N. Singh, H. Trinkhaus, these Proceedings, p. 78.
[41] R. Rauch, J. Peisl, A. Schmalzbauer, G. Wallner, J. Nucl. Mater. 168 (1989) 101.
[42] S.J. Wooding, D.J. Bacon, W.J. Phythian, Phil. Mag. A 72 (1995) 1261.
[43] B. Whiting, D.J. Bacon, in: T. de la Rubia et al. (Eds.), Proceedings of the Symposium on Microstructure Evolution During Irradiation, vol. 439, MRS Pittsburgh, 1997, p. 389.
[44] S.J. Wooding, D.J. Bacon, Philos. Mag. A 76 (1997) 1033.
[45] F. Gao, D.J. Bacon, Yu.N. Osetsky, P.E.J. Flewitt, T.A. Lewis, these proceedings, p. 213.
[46] B.D. Wirth, G.R. Odette, D. Maroudas, G.E. Lucas, J. Nucl. Mater. 244 (1997) 185.
[47] Yu.N. Osetsky, A. Serra, V. Priego, F. Gao, D.J. Bacon, in: Y. Mishin et al. (Eds.), Proceedings of the Symposium on Diffusion Mechanisms in Crystalline Solids, vol. 527, MRS, Pittsburgh, 1998, p. 49.
[48] Yu.N. Osetsky, A. Serra, V. Priego, in: Y. Mishin et al. (Eds.), Proceedings of the Symposium on Diffusion Mechanisms in Crystalline Solids, vol. 527, MRS, Pittsburgh, 1998, p. 59.
[49] Yu.N. Osetsky, V. Priego, A. Serra, B.N. Singh, S.I. Golubov, Philos. Mag. A, submitted.
[50] Yu.N. Osetsky, D.J. Bacon, A. Serra, B.N. Singh, S.I. Golubov, these Proceedings, p. 65.
[51] A.F. Calder, D.J. Bacon, J. Nucl. Mater. 207 (1993) 25.

[52] A.V. Barashev, Yu.N. Osetsky, D.J. Bacon, in: Proceedings of the Symposium on Microstructural Processes in Irradiated Materials, vol. 540, MRS, Pittsburgh, 1999, p. 697.
[53] F. Gao, D.J. Bacon, P.E.J. Flewitt, T.A. Lewis, J. Nucl. Mater. 249 (1997) 77.
[54] F. Gao, D.J. Bacon, in: Proceedings of the Symposium on Microstructural Processes in Irradiated Materials, vol. 540, MRS, Pittsburgh, 1999, p. 661.
[55] M.A. Kirk, M.L. Jenkins, H. Fukushima, these Proceedings, p. 50.
[56] D. Hull, D.J. Bacon, Introduction to Dislocations, 3rd ed., Pergamon, Oxford, 1984.
[57] D.J. Bacon, J. Nucl. Mater. 206 (1993) 249.
[58] Yu.N. Osetsky, D.J. Bacon, A. Serra, Philos. Mag. Lett., 79 (1999) 273.
[59] C.A. English, M.L. Jenkins, Mater. Sci. Forum 15–18 (1987) 1003.
[60] C.A. English, A.J.E. Foreman, W.J. Phythian, D.J. Bacon, M.L. Jenkins, Mater. Sci. Forum 97–99 (1992) 1.
[61] K. Nordlund, R.S. Averback, these Proceedings, p. 194.
[62] Yu.N. Osetsky, M. Victoria, A. Serra, S.I. Golubov, V. Priego, J. Nucl. Mater. 251 (1997) 34.
[63] Yu.N. Osetsky, A. Serra, M. Victoria, V. Priego, S.I. Golubov, Phil. Mag. A, in press.